IEEE Access
Multidisciplinary | Rapid Review | Open Access Journal

Received 19 July 2024, accepted 26 July 2024, date of publication 30 July 2024, date of current version 12 August 2024.

Digital Object Identifier 10.1109/ACCESS.2024.3435741

RESEARCH ARTICLE

Predicting Lane Change and Vehicle Trajectory With Driving Micro-Data and Deep Learning

LEI WANG[1,2], JIANYOU ZHAO[1], MEI XIAO[3], AND JIAN LIU[2]
[1]School of Automobile, Chang'an University, Xi'an, Shaanxi 710061, China
[2]School of Automobile & Rail Transportation, Tianjin Sino-German University of Applied Sciences, Tianjin 300350, China
[3]College of Transportation Engineering, Chang'an University, Xi'an, Shannxi 710061, China

Corresponding author: Lei Wang (wangleidr@chd.edu.cn)

This work was supported in part by Tianjin Transportation Technology Development Plan Project under Grant 2023-7 and Grant 2022-32.

ABSTRACT In the evolving landscape of mixed human-machine driving environments, autonomous vehicles (AVs) confront the challenge of anticipating the lane-changing intentions and subsequent driving trajectories of neighboring vehicles. This capability is essential for optimizing safety, efficiency, and comfort in decision-making processes. This paper introduces a novel hybrid prediction model, the LSTM-GAT-Bilayer-GRU, which leverages deep learning to enhance predictive accuracy and real-time responsiveness in dynamic traffic scenarios. The proposed model consists of two main components: a lane change prediction model (LSTM-GAT) and a trajectory prediction model (G-BiLayer-GRU), to process and predict complex vehicular interactions and environmental dynamics effectively. The efficacy of this integrated model was tested using the HighD dataset for training, validation, and testing purposes. The results of a benchmark analysis indicate that the proposed model demonstrated superior prediction performance and reliability over the Support Vector Machine (SVM), Random Forest (RF), AlexNet and Back-Propagation Through Time (BPTT) in the context of lane change intention recognition. Combining LSTM for temporal data processing with GAT for spatial interaction analysis, along with the GRU's precise trajectory prediction, achieved the best error evaluation metric and balanced prediction time consuming metric under the six prediction time-interval, marks a substantial advancement in AVs technology. This integration guarantees smooth operation of AVs in intricate driving scenarios, fine-tuning their reactions to bolster road safety and passenger comfort.

INDEX TERMS Lane change, vehicle trajectory, prediction, data, deep learning, autonomous vehicle.

I. INTRODUCTION

The integration of autonomous driving and vehicle-road collaborative systems into everyday traffic settings is swiftly transforming the landscape of modern transportation. This mixed traffic environment, where autonomous and human-driven vehicles coexist and interact, is increasingly becoming the norm [1]. Within this context, the fusion of human and machine driving behaviors has emerged as a crucial facet of contemporary traffic dynamics. Understanding the technical intricacies and evolutionary patterns of this human-machine hybrid driving traffic flow is paramount for advancing autonomous driving technology and intelligent transportation systems.

In traditional human-driven scenarios, drivers must continuously assess the surrounding environment, the vehicle's operational status, and adhere to traffic regulations to make informed driving decisions in real-time. However, these decisions are inevitably influenced by factors such as individual driving style, skill level, and subjective cognitive biases, introducing limitations and inherent risks [2], [3]. In contrast, AVs leverage objective environmental data to predict neighboring vehicles' movements and execute optimal driving decisions within predefined constraints, such as lane changes [4]. Thus, the core problem of autonomous driving lies in intelligent decision-making technology, this

The associate editor coordinating the review of this manuscript and approving it for publication was Tariq Umer.

technology enables safe and efficient navigation while effectively managing the complexities and uncertainties of the environment [5].

Consequently, the proficiency of intelligent decision-making technology in navigating complex traffic scenarios has emerged as a key benchmark for assessing the maturity of autonomous driving systems [6]. Notably, research endeavors focusing on human-machine mixed traffic flow, particularly in understanding behaviors related to following and lane changes, have garnered global scholarly attention, reflecting their significance as research frontiers.

Kesting et al. [7] introduced the MOBIL model, which incorporates an acceleration control feature to gauge lane satisfaction based on the driver's anticipated acceleration. This model has shown to influence lane change behaviors to achieve higher satisfaction levels, however, it may not fully capture the complex interactions and dynamics of real-world traffic scenarios. Moridpour et al. [8] developed a fuzzy logic model for lane change decision-making, addressing the impact of heavy truck lane changes on surrounding traffic. While this model has demonstrated positive results and improved macro traffic flow estimations, its application in micro traffic models may still have limitations in accurately predicting lane and vehicle trajectory changes. Xu et al. [9] proposed a comprehensive threat assessment algorithm that considers potential risks posed by nearby vehicles. This algorithm aids decision-making systems in AVs by determining safe trajectories in real-time. Nonetheless, it may not fully account for the dynamic nature of traffic patterns and driver behaviors. Cao [10] explored the adaptability of decision-making models to dynamic environments, utilizing Classification and Regression Trees (CART) and Generative Adversarial Networks (GAN). This approach shows promise but may require further validation in real-world traffic conditions. Wang et al. [11] proposed a decision planning method based on motivation and risk assessment, considering real-time driving behavior and trajectory planning. This method improves decision-making efficiency and ensures safety, but its effectiveness in highly dynamic and unpredictable traffic situations remains to be tested. Jeong [12] developed a lane change decision algorithm using a recurrent neural network (RNN) with Bi-LSTM units. While this algorithm has been trained and validated using data from various sensors, its performance in diverse and complex traffic scenarios has not been extensively evaluated. Hu et al. [13] introduced a probabilistic decision-making and trajectory planning framework for autonomous heavy trucks, which segments the decision-making process into intent generation and feasibility assessment. Their framework demonstrates human-like lane-changing decisions in simulation experiments, but its applicability to different types of vehicles and traffic conditions needs further investigation.

In summary, the current research on vehicle lane change models is primarily based on the theoretical analysis and modeling of human driving behavior, and these studies have achieved certain results in theoretical and experimental environments. However, in order to more accurately simulate and understand human driving behaviors in the real world, and improve the practicality and safety of automatic driving systems, it is particularly important to use standardized and highly reliable large sample road traffic measurement data for parameter calibration and verification. Natural driving datasets, provide rich and realistic traffic scenarios that fully reflect the complex behaviors and interactions of vehicles in real traffic environments. With the help of deep learning technology for effective mining and learning of such interactive behavior, we can more accurately capture the dynamic evolution of vehicles and traffic environment. And then improve the decision-making efficiency and adaptability of the automatic driving system. Therefore, the combination of natural driving data set and deep learning technology is of profound necessity and significance for the advancement and practical application of autonomous driving technology.

Based on the above analysis, the following research contents will be carried out in this paper:

(i) Building the LSTM-GAT-Bilayer-GRU hybrid prediction model for vehicle driving status, which consists of a lane change prediction model (LSTM-GAT) and a trajectory prediction model (G-BiLayer-GRU), to process complex vehicular interactions in human-machine mixed driving traffic flow, and accuratelypredict lane change intentions and driving trajectories of target vehicles under different time intervals.

(ii) Utilizing the Kalman filtering algorithm to refine the HighD dataset firstly; Then, filter and collect vehicle trajectory data based on car classification, lane change time, and lateral displacement offset; Finally, define a starting and end point discrimination model for the vehicle lane changing process to enhance the accuracy and reliability of the original training data.

(iii) Using the extensive natural driving data processed from HighD dataset and the Deep Learning Toolbox learning framework, we will train, validate, and test the LSTM-GAT and G-BiLayer-GRU models. Subsequently, we will conduct a comparative analysis between the proposed model and commonly used models, evaluating them based on error indexes, time-consuming indexes, and classification indexes. The aim is to underscore the notable advantages of the proposed hybrid prediction model in characterizing vehicle dynamic features and enhancing prediction accuracy within complex traffic environments.

II. MODEL FRAMEWORK

In view of the deficiency of traditional models in describing vehicle dynamic feature and the insufficiency of current V2X vehicle-to-road collaboration facilities, this paper proposes an hybrid model, called LSTM-GAT-Bilayer-GRU (shown in Figure 1), integrating the features of Long short-term memory (LSTM), Graph

Attention Network (GAT), and Gate Recurrent Unit (GRU). The LSTM-GAT-Bilayer-GRU model consists of a

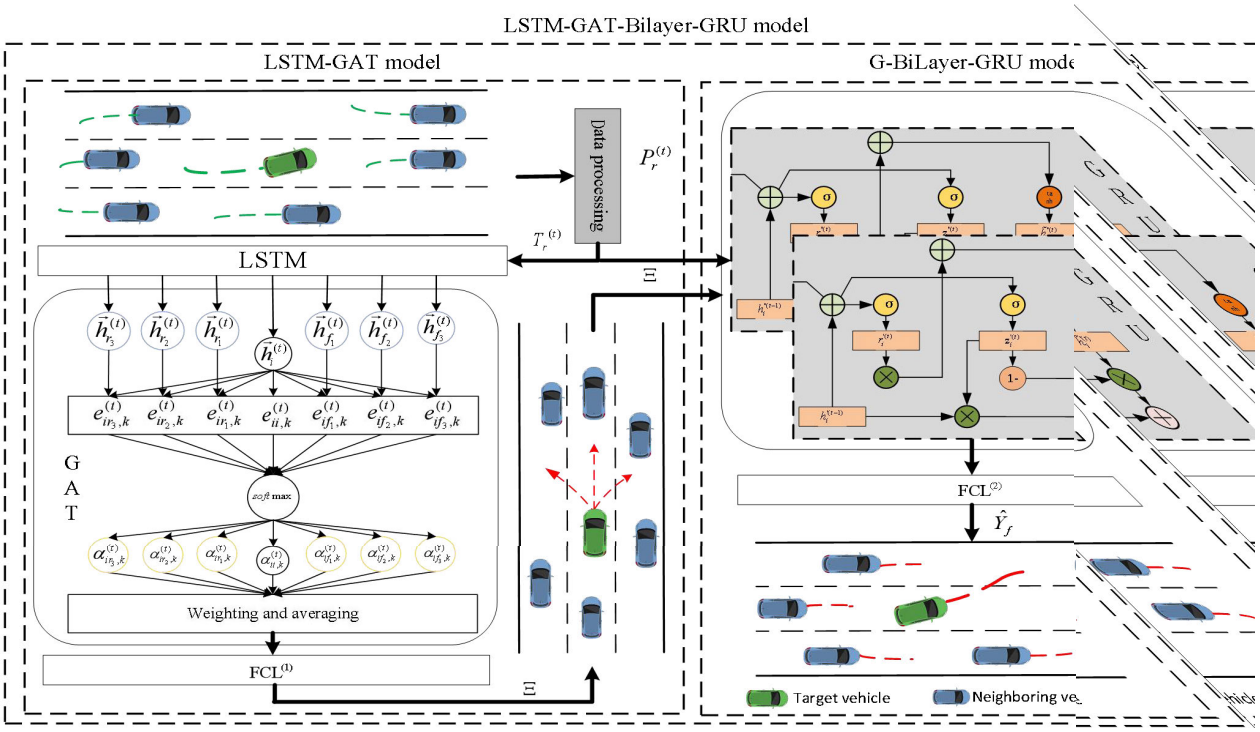

FIGURE 1. Structure of the hybrid prediction model (LSTM-GAT-Bilayer-GRU).

lane change prediction model (LSTM-GAT) and a trajectory prediction model (G-BiLayer-GRU). The LSTM-GAT model is composed of a data pre-processing model, LSTM encoder and GAT decoder, while the G-BiLayer-GRU is composed of an encoder model, a feature splitter model and a decoder model. The fully connected layers ($FCL^{(1)}$ and $FCL^{(2)}$) in the LSTM-GAT-Bilayer-GRU, integrate the high-dimensional feature extracted from the previous network layer and achieve effective dimensionality reduction, and remove redundant information to output the most relevant feature.

The proposed model input, the spatio-temporal trajectory sequence $T_r^{(t)}$ of a target vehicle, can be formulated as Eq. 1 below.

$$T_r^{(t)} = \left[P_r^{(t)}, S^{(t)}\right], t \in (t_P - T_L, t_P - T + 1, \cdots, t_P - 1, t_P) \tag{1}$$

where at time t, $P_r^{(t)}$ is the processed historical state feature of the target vehicle, $S^{(t)}$ is the processed historical feature of the neighboring vehicles in the surrounding environment; T_L is the length of sliding time window [14]; t_P is the end trajectory point of the sliding time window. We set $P_r^{(t)} = [x^{(t)}, y^{(t)}, v_x^{(t)}, v_y^{(t)}, a_x^{(t)}, a_y^{(t)}, \theta^{(t)}, L_p^{(t)}]$ for the target vehicle, wherein $x^{(t)}, y^{(t)}$ is the coordinates; $v_x^{(t)}, v_y^{(t)}$ represent the longitude and latitude speeds; $a_x^{(t)}, a_y^{(t)}$ is the longitude and latitude accelerations; $\theta^{(t)}$ is the heading angle; $L_P^{(t)}$ is the lane position. The vehicles' feature parameters discussed above are illustrated in Figure 2.

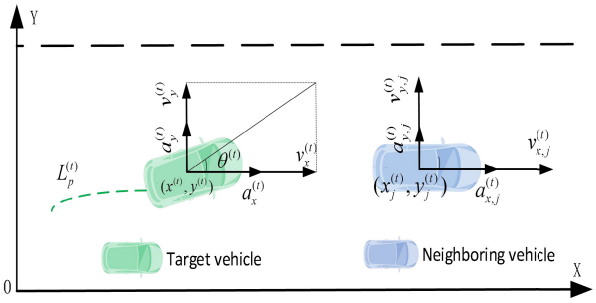

FIGURE 2. Feature information of vehicles.

The neighboring vehicles for the target vehicle consists of six angles: front left (f_1), front (f_2), front right (f_3), back left (r_1), back (r_2)

and back right (r_3). Thus, the six features of the neighboring vehicles $S^{(t)}$ can be expressed as Eq. 2:

$$S^{(t)} = [S_{f_1}^{(t)}, S_{f_2}^{(t)}, S_{f_3}^{(t)}, S_{r_1}^{(t)}, S_{r_2}^{(t)}, S_{r_3}^{(t)}] \tag{2}$$

The attributes of the *j-th* vehicle denoted as $S_j^{(t)}$ include position, speed and acceleration, expressed as Eq. 3:

$$S_j^{(t)} = [x_j^{(t)}, y_j^{(t)}, v_{x,j}^{(t)}, v_{y,j}^{(t)}, a_{x,j}^{(t)}, a_{y,j}^{(t)}], j \in [f_1, f_2, f_3, r_1, r_2, r_3] \tag{3}$$

Input the $T_r^{(t)}$ to the LSTM network layer, LSTM gradually processes the data of each time point in the trajectory time sequence through the input gate, the forgetting gate and the

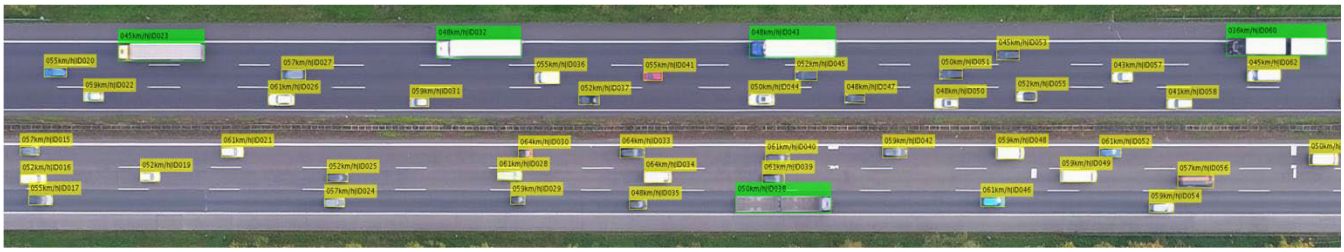

FIGURE 3. Schematic diagram of road section for vehicle data collection in HighD dataset.

output gate, captures the long-term time dependence of the vehicle trajectory through the hidden state H_t and the memory unit state C_t, to obtains the key features. By extracting the output of the last layer of the LSTM network as the feature vector containing the historical trajectory feature, which is input into the GAT model, constant and dynamical iteration process of attention coefficient and feature tensor of target vehicle is executed in the GAT model, finally, $\mathrm{FCL}^{(1)}$ outputs the probability of lane change intent vectors and convert it to $One-hot$ vector according to the default thresholds. At the t_P time, $P_r^{(t)}$ extracted by LSTM and $One-hot$ vector output by $\mathrm{FCL}^{(1)}$ are combined and input into the Bilayer-GRU model to obtain the multi-dimensional predicted trajectory, which is input into $\mathrm{FCL}^{(2)}$ to calculate the final predicted trajectory $\hat{Y}_f = (\hat{x}_f, \hat{y}_f), f \in \left(t_P + 1, t_P + 2, \cdots, t_P + \mathrm{t}_{pred}\right)$, wherein $\hat{x}_f$ and $\hat{y}_f$ are the longitude and latitude coordinates of the vehicle's predicted trajectory; t_{pred} is the advanced prediction intervals. The $\hat{y}_f$ can be optimized by adjusting the appropriate weights and biases of the neural network to bring it as close as possible to the actual trajectory of the vehicle.

III. DATA PROCESSING AND FRAGMENT EXTRACTION

A. DATA SOURCE

HighD is a drone dataset of naturalistic vehicle trajectories on German highways [15], which is suitable for research in vehicle motion trajectory prediction, driving behavior analysis, and autonomous driving decision planning. The total length of the collection section is 420 m, the sampling frequency is 25Hz, and the collection information includes vehicle ID information, vehicle external size, vehicle coordinates, running speed, horizontal/longitudinal vehicle acceleration, and vehicle lane. The origin of the coordinate system of HighD data starts from the upper left, and the position of the vehicle is marked by the upper left end of the bounding box rather than the center point. Figure 3 is a schematic diagram of a collection section [15].

B. DATA PREPROCESSING

To obtain high-quality training data for training the model, this paper employs MATLAB 2023b to filter out trajectory data specifically for non-continuous lane-changing cars in the middle lane, excluding other vehicle types to minimize training interference, then collects data of neighboring vehicles at each trajectory point to construct a dataset, classified them based on driving behavior (shifting left, moving straight, shifting right), and labels them accordingly with lane information.

For observation data with random errors and measurement noise in a system, the filtering technologies commonly used to improve data quality include moving average method [16], local polynomial method [17], wavelet analysis [18] and Kalman filter [19], [20]. Since the HighD dataset has processed the position, velocity and acceleration of the vehicle in the X and Y coordinate directions before publication, the Rauch-Tung-Striebel (RTS) algorithm (Under the Kalman filter framework) and the uniform acceleration model are used to refine the vehicle trajectory, thus greatly reducing the error and sensors' white noise. After inspection with the algorithm of wavelet analysis and physical constraint limit values [21], the acceleration in the dataset is within the range of -3 m/s^2 to 3 m/s^2, which is in line with vehicles performance and human tolerance, with small fluctuation range and smooth curve, so it is no longer necessary to smooth the trajectory data of the HighD dataset [22]. As a example in this paper, longitude and lateral accelerations data of a lane change vehicle at 8:38 on Tuesday, September 2017, are shown as Figure 4 (a) and (b). In Table 1, it shows the data for a car in the middle lane at 8:21 AM on Monday, September 2017. The first 8 columns show the raw data of the HighD dataset which is the real-time observation value of the vehicle in driving state, such as the position, speed and acceleration of the vehicle. The last 12 columns of data is the relative spatial distance between the target vehicle and the neighbor vehicles deduced from the raw data.

C. DATA FILTERING

(i) The HighD dataset comprises both cars and trucks. Notably, trucks predominantly drive in the right lane and rarely change lanes compared to cars. To accurately represent the lane-changing behaviors of vehicles on highways, only the driving data of cars are selected from the dataset.

(ii) The vehicle trajectory data in the dataset is recorded in a time series and includes many instances of abnormal lane changes. To isolate trajectories that represent typical lane changes, we impose constraints on the duration of the lane change, which must not exceed 8 seconds, and the vehicle must remain in the new lane for at least 10 seconds following the lane change. A lateral displacement of less than

TABLE 1. Vehicle trajectory data of HighD dataset after processing.

Frame Sequence	Vehicle ID	X Coordinate	Y Coordinate	X Velocity	Y Velocity	X Acceleration	Y Acceleration	Distance with f_2		Distance with f_1		Distance with f_3		Distance with r_2		Distance with r_1		Distance with r_3	
								x	y	x	y	x	y	x	y	x	y	x	y
282	28	111.25	23.82	31.79	0.05	0.13	-0.01	78.66	0.47	36.03	3.78	31.55	3.11	107.71	0.24	6.37	3.55	56.49	3.14
283	28	112.52	23.82	31.80	0.05	0.13	0.01	78.99	0.45	36.35	3.77	31.26	3.11	107.81	0.23	6.00	3.54	56.76	3.15
284	28	113.80	23.82	31.80	0.04	0.13	-0.01	79.30	0.43	36.68	3.77	30.96	3.11	107.87	0.22	5.63	3.54	57.04	3.15
285	28	115.07	23.83	31.81	0.04	0.14	-0.01	79.62	0.42	37.01	3.78	30.67	3.10	107.89	0.22	5.26	3.55	57.31	3.15
286	28	116.34	23.83	31.82	0.04	0.14	-0.01	79.92	0.40	37.34	3.77	30.38	3.11	107.89	0.21	4.89	3.54	57.58	3.16
287	28	117.61	23.83	31.82	0.04	0.14	-0.01	80.22	0.38	37.67	3.77	30.08	3.11	107.87	0.20	84.91	3.74	57.85	3.16
288	28	118.88	23.83	31.83	0.04	0.14	-0.01	80.52	0.36	38.00	3.77	29.79	3.11	107.86	0.19	84.45	3.73	58.13	3.17
289	28	120.15	23.83	31.83	0.04	0.15	-0.01	80.84	0.34	38.33	3.77	29.52	3.11	107.83	0.18	83.99	3.71	17.81	3.34
290	28	121.43	23.83	31.84	0.04	0.15	-0.01	81.15	0.32	38.66	3.76	29.23	3.12	107.80	0.17	83.54	3.70	18.10	3.34
291	28	122.71	23.84	31.84	0.04	0.15	-0.01	81.46	0.31	38.99	3.77	28.94	3.11	107.77	0.18	83.10	3.70	18.39	3.33

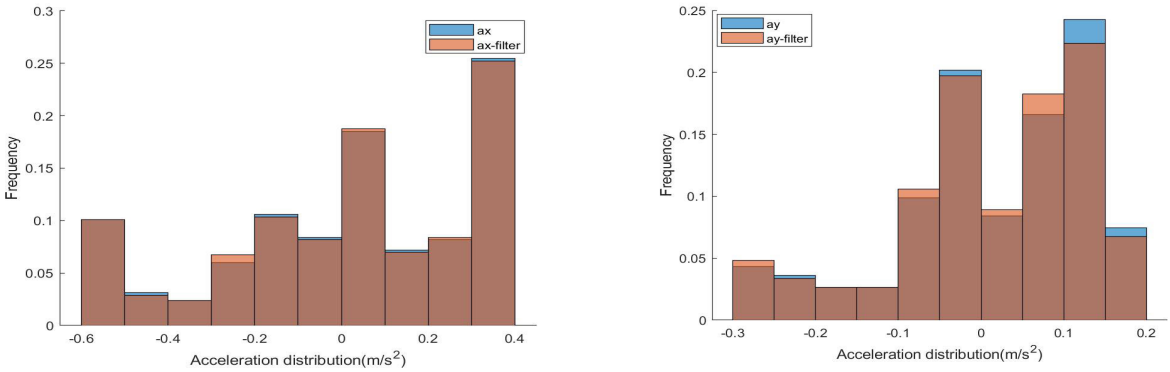

(a) Statistical information of longitude acceleration

(b) Statistical information of latitude acceleration

FIGURE 4. Acceleration feature data of sample vehicle.

0.5 meters during the trajectory collection is classified as non-lane change behavior.

(iii) From the dataset, a total of 4,191 sets of vehicle trajectory data were filtered, consisting of 2,123 sets involving lane changes and 2,068 sets without lane changes.

D. EXTRACTION OF DATA FRAGMENTS

In order to better study lane change prediction model, it is necessary to focus on the starting and ending point data of vehicle trajectory. For a single lane change trajectory in the HighD dataset, it is necessary to extract the starting point of lane change and the corresponding characterization parameters of the starting point time. In order to avoid misjudgment and interference on the starting point of lane change caused by small lateral displacement of the vehicle or continuous lane change, the lateral displacement and trajectory curvature of the vehicle are used as the judging criteria for whether the vehicle changes lane. For a single complete lane change process, the lateral displacement and trajectory curvature at the starting and ending point of the lane change should meet the Eq. 4.

$$\begin{cases} L - D \leq \mid y(t + c_t) - y(t) \mid \leq L + D \\ k(t + ct) = k(t) \leq k_{t0} \end{cases} \tag{4}$$

In Eq. 4, $y(t)$ is the lateral position of the vehicle at the t time; c_t is the lane change time; L is lane width; D is the lateral displacement offset; $k(t)$ is the slope of vehicle driving trajectory at the t time; k_{t0} is the slope threshold of the starting point of lane change.

For the change prediction model, it is necessary to divide the extracted trajectory fragments into three classification as shifting left, shifting right and straight-line driving, and label

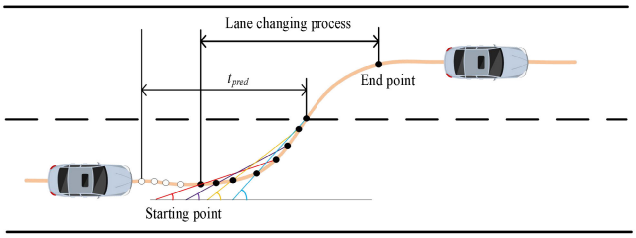

FIGURE 5. Definition of critical trajectory for lane change process.

the three categories. In this paper, the starting point and end point of lane change are determined as follows:

(ii) The intersection point of vehicle trajectory and lane line is defined as the lane change point.

(ii) Calculate the slope $k_t = \frac{y_t - y_{t-4}}{x_t - x_{t-4}}$ between the position (x, y) at t time and the position (x_{t-4}, y_{t-4}) at $t-4$ time of the vehicle trajectory. This calculation method can eliminate the problem of unclear slope differences between adjacent points caused by dense sampling and noise in the HighD dataset.

(iii) The slope k_j of each sampling point is traversed from the lane change point to both the positive and negative directions. If the trajectory time sequence has 4 consecutive sampling points $|k_j| \geq k_{t0}$, the position that reaches the threshold k_{n0} for the first time is positioned as the starting point of the lane change, and the ending point of the lane change is determined in the same way, and the continuous four-point confirmation here is to avoid misjudgment caused by noise. The points between the start and end of the lane change are defined as the lane changing process points, as shown in Figure 5.

In this paper, the sliding time window method is employed to extract the trajectory time sequence of the specified length, and 15 sampling points are updated forward each time. Let the length of the intercepted sequence be n sampling points, then the information of $n - 15$ trace points in the adjacent two sequences is the same. The method of sliding time window can maximize the use of data. The sampling frequency is 25Hz, when the time domain of the input sequence is the length of the sliding time window T_L, then the length of the trajectory time sequence is $n = 25T_L$. If the extracted trajectory time sequence contains the lane changing process points, the sequence is marked as the trajectory time sequence of lane change; otherwise, it is the trajectory time sequence of moving straight driving. This paper labels the lane change of shifting left as '1', moving straight as '2', shifting right as '3', to meet the requirement of deep learning models.

IV. LANE CHANGE PREDICTION MODEL

The lane change process is a comprehensive behavior process in which the driver adjusts the decision intent and completes the driving goal strategy by estimating the vehicle operating environment and vehicle operating state [23]. In this paper, the lane change prediction model consists of data processing model, LSTM encoder, GAT decoder and FCL$^{(1)}$ output layer.

After preprocessing steps such as normalization, data tiling, and format conversion, the spatio-temporal trajectory sequence $T_r^{(t)}$ of the target vehicle is obtained, then it is then input into the LSTM for encoding, outputting the target vehicle's historical trajectory feature vector $L^{(t)}$ at time t. The mathematical principle is shown in Eq. 5, wherein $W^{(t)}$ is the weight parameter of the LSTM.

$$L^{(t)} = LSTM\left(L^{(t-1)}, T_r^{(t)}, W^{(t)}\right) \tag{5}$$

The attention mechanism model comes from people's visual attention mechanism, people usually use their limited attention to get the most effective information from a large number of information sources [24]. Due to the different driving state parameters and sizes of neighboring vehicles, the interaction effects of target vehicles under the same Euclidean distance are different, so the conventional Euclidean distance models cannot describe the complex spatial interaction feature between vehicles well. In this paper, a novel type of spatial interaction relationship is defined. Considering the factors such as coordinate component $x^{(t)}, y^{(t)}$, velocity component v_x, v_y, acceleration component a_x, a_y, a spatial interaction topology is established between the target vehicle and the neighboring vehicles, and the adjacency matrix is used to express this complex topological relationship. The feature vector $\mathrm{L}^{(t)}$ extracted from the LSTM is dimensionally reduced and normalized, and then input into GAT model as point feature to capture the complex spatial interaction relationship between the target vehicle and the neighboring vehicles at any t time, then generate the spatial-temporal feature tensor representing the structural information of the topological graph, $\vec{H}^{(t)} = \{\vec{H}_i^{(t)}, \vec{H}_j^{(t)}\}, \vec{H}_i^{(t)} \in R^F, \vec{H}_j^{(t)} \in R^F$, wherein $H_j^{(t)}$ is the point feature tensor of the neighboring vehicles; F is the feature dimension; R is real number. Namely, the vehicle feature information of six directions for the target vehicle: front left (f_1), front (f_2), front right (f_3), back left (r_1), back (r_2) and back right (r_3). In order to better capture the interaction between the target vehicle and the neighboring vehicles, the original space-time feature tensor $\vec{H}^{(t)}$ is mapped to a new feature space by the use weight matrix $W_H^{(t)} : R^{F' \times F}$, and splice new vehicle feature vectors. Then, according to the degree of multi-dimensional influence of neighboring vehicles on target vehicles, the corresponding influence coefficient $e_{ij,k}^{(t)}$ is calculated by multi-head $a_k^{(t)} : R^{F'} \times R^{F'}$, wherein k is the number of attention heads [25], k attention heads calculate different attention coefficients and calculate their average to get the final attention coefficient. Each attention head independently calculates the influence coefficients of different factors which are normalized by *LeakyRelu* nonlinear activation function and *soft* max function to get the attention coefficient $\alpha_{ij,k}^{(t)}$ reflecting the importance of different neighboring vehicles to the target vehicle, wherein, the LeakyRelu function is used to alleviate the gradient disappearance and enhance the nonlinear expression of the model, and the attention coefficient is obtained by the normalization of the softmax

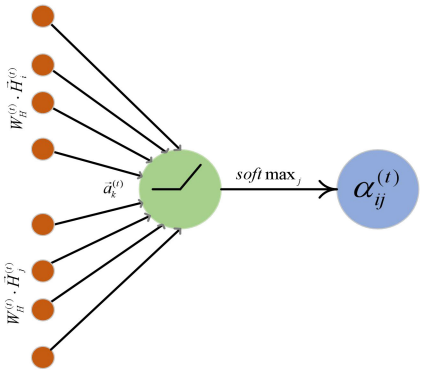

FIGURE 6. Calculation process of influence coefficient of attention mechanism.

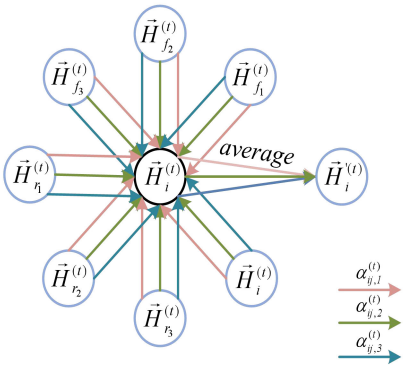

FIGURE 7. Update process of target vehicle features.

function, as shown in Figure 6. Utilizing $\alpha_{ij,k}^{(t)}$ as weights, the weighted summation of the transformed point feature tensors of neighboring vehicles is executed to obtain the aggregate features that fuse the information of neighboring vehicles, and then update the feature matrix $H_i^{\prime(t)}$ of target vehicles in future time, as shown in Figure 7. The updating calculation process of influence coefficient $e_{ij,k}^{(t)}$, attention coefficient $\alpha_{ij,k}^{\prime(t)}$ and feature matrix $H_i^{\prime(t)}$ is shown in Eq. 6, 7 and 8. Then, as the output of GAT model, $H_i^{(t)}$ was transmitted to FCL$^{(1)}$.

$$e_{ij,k}^{(t)} = LeakyReLU\left(a_k^{(t)}\left[W_H^{(t)} \cdot \overrightarrow{H}_i^{(t)} || W_H^{(t)} \cdot \overrightarrow{H}_j^{(t)}\right]\right) \quad (6)$$

$$\alpha_{\mathrm{ij,k}}^{(t)} = softmax_k(e_{ij,k}^{(t)}) = \frac{\exp\left(e_{ij,k}^{(t)}\right)}{\sum_{k=1}^{3}\exp\left(e_{ij,k}^{(t)}\right)} \quad (7)$$

$$\vec{H}^{\prime(t)} = \sigma\left(\frac{1}{k}\sum_{k=1}^{3}\sum_{j=1}^{6}\alpha_{ij,k}^{(t)} \bullet W_H^{(t)} \bullet \vec{H}_{tj}^{(t)}\right) \quad (8)$$

Finally, processed by FCL$^{(1)}$, the lane change intent vector $\Xi = (\xi_1, \xi_2, \xi_3)$ of target vehicle is obtained, wherein ξ_1, ξ_2, ξ_3 is the probability of shifting left, moving straight and shifting right respectively. Making decisions according to the probability of lane change intents calculated by the model above, will lead to low reliability prediction for target vehicle trajectories. In order to improve the prediction confidence of the model, a threshold based on logical decision mechanism is introduced, and the conviction threshold of shifting left and shifting right is set as 85%, moving straight is set as 75%.The lane change intent exceeding the corresponding threshold is regarded as the driver's definite intent, and the probability of the corresponding classification is adjusted to 100%, and the remaining two probabilities are reduced to 0, convert Ξ into $One-hot$ vector to ensure high decisiveness in the model output. In the case that the threshold is not reached, the original probability distribution is maintained to keep the original uncertainty assessment of the lane change intent. This method aims to optimize the prediction accuracy and practicality of the model through threshold judgment, and enhance the ability of intelligent driving systems to cope with complex environments.

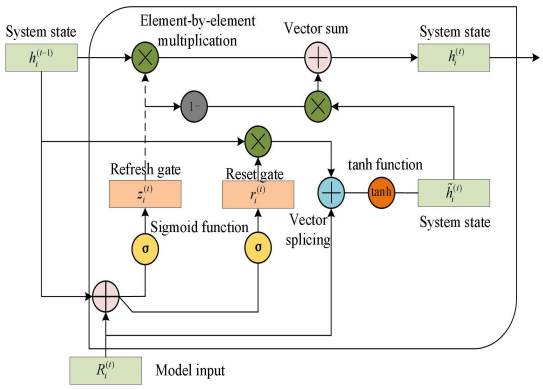

FIGURE 8. Internal working mechanism of GRU model.

V. VEHICLE TRAJECTORY PREDICTION MODEL

Gate Recurrent Unit (GRU) has similar prediction effect with LSTM model but with simpler internal structure, and would greatly improve efficiency in training and prediction. In order to ensure real-time and safety in vehicle trajectory prediction, GRU is preferred, and the internal working mechanism of GRU model is shown in Figure 8.

Combined with the prediction results of LSTM-GAT model, we propose the G-BiLayer-GRU model to predict the future trajectory of vehicles. In order to effectively capture more complex historical vehicle sequence features and time dependence, the two-layer GRU (Bilayer-GRU) model is employed to increase the depth of the network. In the Bilayer-GRU model, the first layer may learn fundamental features about the trajectory (such as changes in lane changing intention, speed and direction), and the second layer may capture more advanced patterns (such as long-term trends or cyclical patterns in driving behavior).

In order to make the decoder output trajectory prediction based on intent prediction, a new trajectory coding tensor $R_i^{\prime(t)}$ is obtained by combining the $One-hot$ vector of lane change intent from the GAT model.

The trajectory coding tensor $R_i^{\prime(t)}$ is used as input, it is transmitted to the first level Gate Recurrent Unit (GRU′). At this level, the GRU′ is responsible for processing the feature tensor of each time step in the sequence and updating its internal hidden state in real time. For each time step in the feature tensor, the GRU′ accepts the input feature of the current time step and the hidden state of the previous time step as a joint input, then calculate the hidden state $h_i^{\prime(t)}$ of the current time step by $z_i^{\prime(t)}$(refresh gate, $r_i^{\prime(t)}$(reset gate) and $\tilde{h}_i^{\prime(t)}$ (system state) to capture the timing dependency in the feature tensor. By extracting useful information from the input through $z_i^{\prime(t)}$ and filtering out useless information and noise, the current hidden state is updated to capture short-term dependencies in time-series data. $r_i^{\prime(t)}$ retains historical vehicle feature information that is useful for the future, thereby capturing long-term dependencies in time sequences. $\tilde{h}_i^{\prime(t)}$ combines the current input and filtered historical information to generate a candidate hidden state. The hidden state uses the update gate to measure the importance of the previous hidden state and the candidate hidden state for forgetting and updating to obtain the final hidden state at the current moment. The aforementioned calculation process is shown in Eq. 9-12.

$$z_i^{\prime(t)} = \sigma(W_z^{\prime} \cdot [h_i^{\prime(t-1)}, R_i^{\prime(t)}]) \tag{9}$$
$$r_i^{\prime(t)} = \sigma(W_r^{\prime} \cdot [h_i^{\prime(t-1)}, R_i^{\prime(t)}]) \tag{10}$$
$$\tilde{h}_i^{\prime(t)} = \tanh(W_h^{\prime(t)} \cdot [r_i^{\prime(t)} \odot h_i^{\prime(t-1)}, R_i^{\prime(t)}]) \tag{11}$$
$$h_i^{\prime(t)} = (1 - z_i^{\prime(t)}) \odot h_i^{\prime(t-1)} + z_i^{\prime(t)} \odot \tilde{h}_i^{\prime(t)} \tag{12}$$

In Eq. 9-12, $z_i^{\prime(t)}$ is the update gate, which is used to control the inflow of information; $r_i^{\prime(t)}$ is the reset gate; $\tilde{h}_i^{\prime(t)}$ is the candidate hidden state, and the input information $R_i^{\prime(t)}$ of the current moment is reserved with the hidden state $h_i^{\prime(t-1)}$ of the previous moment; $h\prime_i^{(t)}$ is the hidden state of the current moment; $W_z^{\prime}$, $W_r^{\prime}$ and $W_{\mathrm{h}}^{\prime(t)}$ is the weight matrix; σ is a *sigmoid* function that changes data into a value between 0 to 1; tanh changes the data to a value between -1 to 1.

The output of the GRU′ is the hidden state of each time step, *dropout* operation is executed to randomly "discard" partial feature of the vehicles to obtain a new feature tensor $R_i^{\prime\prime(t)}$, to serve as the input of the second layer Gate Recurrent Unit (GRU″). At each time step, GRU″ accepts the hidden state from GRU′ as an external input, and combined with the hidden state of its own previous time step, then GRU″ updates the hidden status of the current time step through its internal department control mechanism. GRU″ captures higher levels of time dependence and patterns because it is further analysis and learning based on GRU′'s processing of input sequences and feature extraction. The calculation process of GRU″ is shown in Eq. 13-17.

$$R_i^{\prime\prime(t)} = h_i^{\prime(t)} \cdot \delta_{dropout} \tag{13}$$
$$z_i^{\prime\prime(t)} = \sigma(W_z^{\prime\prime} \cdot [h_i^{\prime\prime(t-1)}, R_i^{\prime\prime(t)}]) \tag{14}$$
$$\mathrm{r}_i^{\prime\prime(t)} = \sigma(W_r^{\prime\prime} \cdot [h_i^{\prime\prime(t-1)}, R_i^{\prime\prime(t)}]) \tag{15}$$
$$\tilde{h}_i^{\prime\prime(t)} = \tanh(W_h^{\prime\prime(t)} \cdot [r_i^{\prime\prime(t)} \odot h_i^{\prime\prime(t-1)}, R_i^{\prime\prime(t)}]) \tag{16}$$
$$h_i^{\prime\prime(t)} = (1 - z_i^{\prime\prime(t)}) \odot h_i^{\prime\prime(t-1)} + z_i^{\prime\prime(t)} \odot \tilde{h}_i^{\prime\prime(t)} \tag{17}$$

In Eq. 13-17, wherein $\mathrm{z}_i^{\prime\prime(t)}$, $r_i^{\prime\prime(t)}$, $\tilde{h}_i^{\prime\prime(t)}$, $R_i^{\prime\prime(t)}$, $h_i^{\prime\prime(t-1)}$, $h_i^{\prime\prime(t)}$, $W_z^{\prime\prime}$, $W_r^{\prime\prime}$ and $W_{\mathrm{h}}^{\prime\prime(t)}$ with the same definition as Eq.9-12; $\delta_{dropout}^{(t)}$ is *dropoutlayer*, some output of GRU′ layers neurons is randomly discarded before input GRU″, which helps to prevent overfitting and improve the generalization performance of the model. In the G-Bilayer-GRU model, each layer is extracting and transforming information, making the data flow from input to output show the feature of deeper by deeper, so that the model can capture complex and multi-dimensional time dependence.The 8-dimensional predicted trajectory of the target vehicle output by the GRU″ is transmitted to the FCL$^{(2)}$ for dimensionality reduction. Finally, processed by FCL$^{(2)}$, output the 2-dimensional predicted trajectory $\hat{Y}_f$ of the target vehicle in the future moment under different lane change decisions.

VI. EXPERIMENT AND ANALYZE

A. CONFIGURATION OF EXPERIMENTAL ENVIRONMENT

(i) The feature data presented in this paper comprises 198,397 sets for shifting left, 265,244 sets for moving straight, and 70,422 sets for shifting right, totaling a comprehensive dataset.

(i) Parameters of related modes, LSTM accepts 44-dimensional vector input, which include 8-dimensional vector of target vehicle and 36-dimensional vector of neighboring vehicles, 128 neurons to capture timing dependencies is adopted, and output 44-dimensional coding vector. Both GRU′ and GRU″ accept an 8-dimensional feature vector of vehicles as input, 128 neurons are used and outputs 8-dimensional vector. FCL$^{(1)}$ accepts the 8-dimensional vector output by the GAT as its input, single hidden layer with 128 neurons, Xavier weight initialization, offset is initialized to 0, *softmax* activation function, Elastic Net regularization, output 3-dimensional vector. FCL$^{(2)}$ accepts the 8-dimensional vector output by the GRU″ as its input, with single hidden layer of 128 neurons, Xavier weight initialization, offset is initialized to 0, no activation function, Elastic Net regularization, output 2-dimensional vector.

(iii) The prediction models are trained with Window10, MATLAB R2023b, Intel Xeon W-2295 CPU, NVIDIA RTX A2000 GPU. Using Deep Learning Toolbox 23.2 as the learning framework. The paper balanced model performance and efficiency by selecting hyperparameters guided by theory and empirical optimization. Learning Rate (0.001) balances convergence speed and stability, commonly used in deep learning. Batch Size (128) compromises gradient accuracy and training efficiency, often yielding good generalization. Dropout Rate (0.2) mitigates overfitting, enhancing robustness without hindering learning. Training Epochs (500 rounds) ensured convergence based on cross-validation, monitoring early stopping to avoid overtraining.

TABLE 2. Confusion matrix of lane chane intent prediction.

True Intent		Shifting Left					Moving Straight					Shifting Right				
		LSTM-GAT	SVM	RF	AlexNet	BPTT	LSTM-GAT	SVM	RF	AlexNet	BPTT	LSTM-GAT	SVM	RF	AlexNet	BPTT
Predictive Intent	Shifting Left	26281	20109	22907	21713	22948	3564	10383	7241	5294	3840	49	148	84	62	124
	Moving Straight	3156	9204	6475	7553	6441	45936	38127	41831	44295	45363	472	1023	788	913	815
	Shifting Right	73	197	128	144	121	685	1675	1113	1296	982	3594	2944	3243	3140	3176

TABLE 3. Performance test of different drive intent prediction models.

Evaluate Indicators	Precision Rate					Recall Rate					F1- Score					Accuracy Rate				
	LSTM-GAT	SVM	RF	AlexNet	BPTT	LSTM-GAT	SVM	RF	AlexNet	BPTT	LSTM-GAT	SVM	RF	AlexNet	BPTT	LSTM-GAT	SVM	RF	AlexNet	BPTT
Shifting Left	0.88	0.66	0.76	0.80	0.85	0.89	0.68	0.78	0.74	0.78	0.88	0.67	0.77	0.77	0.81					
Moving Straight	0.93	0.79	0.85	0.84	0.86	0.92	0.76	0.83	0.88	0.90	0.92	0.77	0.84	0.86	0.88	0.90	0.73	0.81	0.83	0.85
Shifting Right	0.83	0.61	0.72	0.69	0.74	0.87	0.72	0.79	0.76	0.77	0.85	0.66	0.75	0.72	0.76					

For robust model evaluation, we systematically split the HighD dataset into 8:1:1 for training, validation, and testing. The validation set tunes hyperparameters and monitors unseen data performance to prevent overfitting. Early stopping halts training if validation loss stagnates, preserving generalization capabilities.

B. COMPARATIVE ANALYSIS OF MODELS

(i) Comparison of lane change intent models

Early traditional research on lane change prediction mainly focused on the application of physical or rule-based models [26], by assuming the applicability of physical models and using Kalman filter [27], Bayes [28], Decision Tree [29], Support Vector Machine [30], Random Forest [31] and other models, vehicle lane change intention recognition was executed. However, when the forecast time interval is longer, the error of lane change prediction based on physical or rule model will increase as the uncertainty of vehicle trajectory will be greatly increased.

The performance of the lane change prediction model directly affects the quality of trajectory prediction. In order to test the performance of the LSTM-GAT model proposed in this paper, the commonly used models of SVM classifier, RF, AlexNet and BPTT are taken as the benchmark algorithm, and the Accuracy Rate, Recall Rate, F1-Score and Precision Rate were compared. Taking the sliding time window T_L =3s as an example, the performance of LSTM-GAT, SVM, RF, AlexNet and BPTT models for lane change intent is compared and analyzed. Table 2 is the confusion matrix of lane change intent prediction, and Table 3 is the performance test of the different drive intent prediction models.

As can be seen from Table 3, the LSTM-GAT model presents better prediction performance than traditional machine learning models of SVM classifier and RF, common deep learning models of AlexNet and BPTT in the recognition of all lane change intents: shifting left, moving straight and shifting right. Through comparative analysis, the LSTM-GAT model is superior to the comparison model in key evaluation indexes such as Precision Rate, Recall Rate, F1 Score and Accuracy Rate, which verifies the effectiveness and reliability of the model.

In the recognition of shifting left intent, the Precision Rate of LSTM-GAT is 0.88, which is 33.95% higher than SVM, 16.02% higher than RF, 21.04% higher than AlexNet and 14.52% higher than BPTT. The Recall Rate of LSTM-GAT was 0.89, which was 30.70% higher than SVM, 14.74% higher than RF, 9.60% higher than AlexNet and 3.10% higher than BPTT. The F1 Score of LSTM-GAT was 0.88, compared with SVM improved by 32.34%, compared with RF improved by 15.37%, compared with AlexNet improved by 15.28%, and compared with BPTT improved by 8.78%. The F1 Score is the balanced average of accuracy and Recall Rate, and a higher F1 Score indicates that LSTM-GAT achieves a better balance between accuracy and comprehensiveness.

In moving straight intent prediction, the Precision Rate of LSTM-GAT is 0.93, which is 17.54% higher than SVM and 8.8% higher than RF, 3.70% higher than AlexNet and 1.26% higher than BPTT. The Recall Rate of LSTM-GAT was 0.92,

which was improved by 20.48% compared with SVM and 9.81% compared with RF, 10.39% higher than AlexNet and 7.50% higher than BPTT. The F1 Score of LSTM-GAT was 0.92, compared with SVM improved by 19.02%, compared with RF improved by 9.29%, compared with AlexNet improved by 7.03% and compared with AlexNet improved by 4.36%; It further confirms the superiority of LSTM-GAT in the accuracy and comprehensiveness of moving straight intent prediction.

In shifting right intent prediction, the Precision Rate of LSTM-GAT is 0.83, which is 35.09% higher than SVM and 14.19% higher than RF, 14.46% higher than AlexNet and 13.16% higher than BPTT. The Recall Rate of LSTM-GAT was 0.87, which was 22.09% higher than SVM and 10.82% higher than RF, 20.46% higher than AlexNet and 11.26% higher than BPTT. The F1 Score of LSTM-GAT was 0.85, compared with SVM improved by 28.76%, compared with RF improved by 12.54%, compared with AlexNet improved by 17.54%, and compared with BPTT improved by 12.19%. It shows its high efficiency and accuracy in recognizing intent of shifting right.

Due to the interaction between vehicles and the high complexity and uncertainty of traffic environment, lane change prediction of vehicles has a highly complex nonlinear feature. SVM can select appropriate kernel function to deal with nonlinear problems, but compared with RF and GAT, SVM is not effective in predicting driving intent affected by various factors. The basic classifier of RF is a decision tree that adopts the decision-making method of a single classifier, which is more likely to fall into the local optimal solution. In the processing of massive data, due to the imbalance of data set classification, it is easy to prefer the classification with a large number of samples, resulting in a decrease in the prediction accuracy of the model. AlexNet and BPTT models excel in data processing capabilities, but their limited ability to handle time sequences data results in their inability to achieve the level of performance in lane change intention prediction demonstrated by the model proposed in this paper. The superior performance of LSTM-GAT model compared to SVM and RF across multiple metrics is due to its proficiency in efficiently handling time series data, capturing long-term temporal dependencies, and leveraging a graph attention mechanism to prioritize crucial features, ultimately enhancing the accuracy and robustness of lane change prediction.

According to relevant literature, in a highway environment, the duration of a lane change is generally between 3.5 and 6.5 s, with an average of 5 seconds being sufficient for a complete lane change process [32]. The change prediction model can ''observe'' the road condition and ''understand'' the changing law of the traffic environment from the view of the target vehicle, and make reasonable prediction in advance. Now, a representative complete trajectory time sequence of shifting left (the 28th shifting left vehicle; middle lane; y-axis forward; the 34th day) is selected from the test dataset, and the lane change prediction model proposed in this paper is applied to conduct dynamic pattern recognition of the driving behavior for the target vehicle, as shown in Figure 9. 4s after the target vehicle has departed from the starting point of the trajectory, the LSTM-GAT model recognizes that the vehicle is likely to shift left. At this time, the probability ξ_1 of shifting left increases somewhat, but the condition of lane change point is far from being met, so the probability increases slightly. When the target vehicle drives to the position 2s away from the lane change point, the LSTM-GAT model predicts that the vehicle will take a shifting left behavior. At this time, the probability of shifting left ξ_1 starts to rise rapidly, but it does not reach 85% of the certainty threshold, so output the three classification of probabilities $\Xi = (\xi_1, \xi_2, \xi_3)$ derived from the FCL$^{(1)}$ layer. When the target vehicle travels to the position 1s away from the lane change point, the model recognizes that the probability of shifting left ξ_1 has exceeded 85%, and the corresponding probability is adjusted to 1. At this time, the probabilities of shifting left, moving straight and shifting right output by LSTM-GAT are $\Xi = (1, 0, 0)$, and the trajectory output model only outputs one type of position distribution. When the target vehicle reaches the end point of lane changing process, the recognition of shifting left intent rapidly decreases to 0, the intent probability of moving straight ξ_2 rapidly increases to 1, and the probability returns to the initial state $\Xi = (0, 1, 0)$.

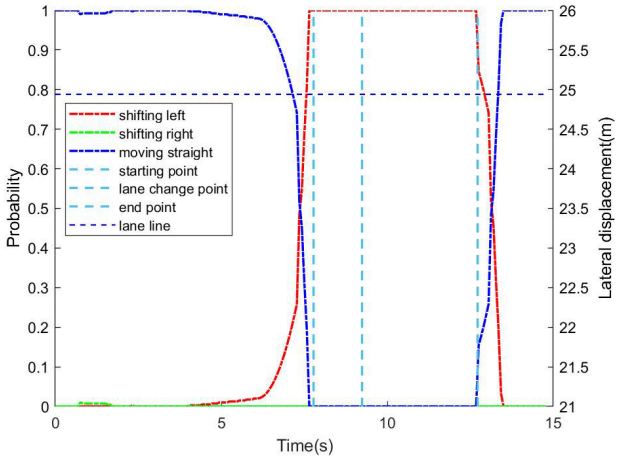

FIGURE 9. Probability conversion diagram of lane change intent.

(ii) Comparison of trajectory prediction models

In order to comprehensively evaluate the performance of the G-BiLayer-GRU model in vehicle trajectory prediction, longitudinal and horizontal comparison verification methods are used in this paper. In the longitudinal comparison verification of this paper, six different advanced prediction intervals (called t_{pred} in this paper, shown in Figure 5) of 3.0s, 2.5s, 2.0s, 1.5s, 1.0s, and 0.0s were selected to the opposite direction of vehicle travel by taking the lane change point as the reference point, to observe the prediction effect of the model in different t_{pred}. In the horizontal comparison, this paper selected five common trajectory prediction models, including Triple layer

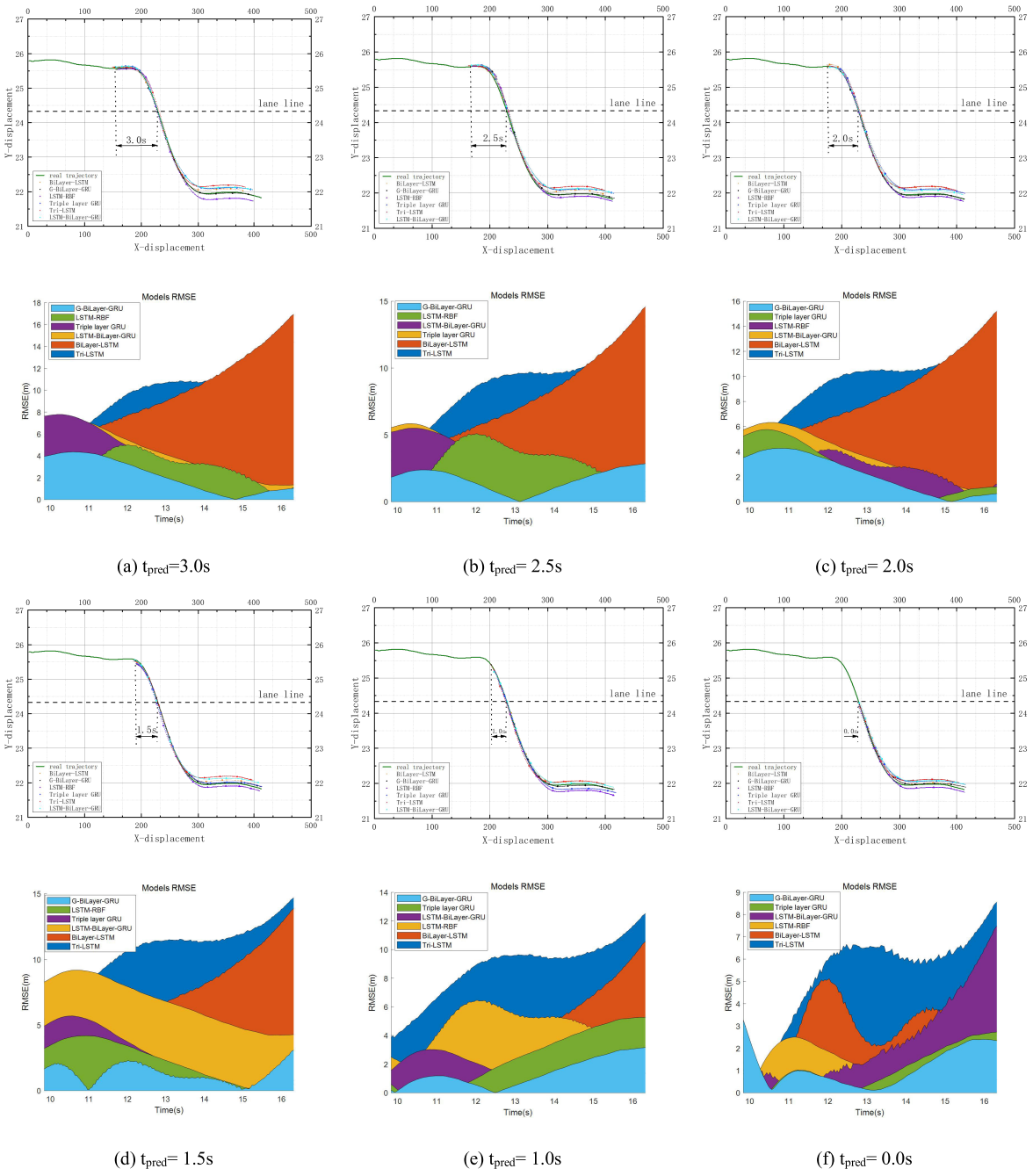

(a) t_{pred}=3.0s (b) t_{pred}= 2.5s (c) t_{pred}= 2.0s

(d) t_{pred}= 1.5s (e) t_{pred}= 1.0s (f) t_{pred}= 0.0s

FIGURE 10. Trajectory scatter at different advanced prediction intervals.

GRU [33], LSTM-BiLayer-GRU, BiLayer-LSTM [34], Tri-LSTM [35] and LSTM-RBF [36], and compared them with G-BiLayer-GRU by using RMSE(Root Mean Square Error), ADE(Average Displacement Error), FDE (Final Displacement Error) and prediction time consuming(called PTC in this paper) as the evaluation indexes.

In practical applications, the trajectory prediction models of the AVs need to have the ability to predict the future trajectory distribution of the target vehicle in real time. Therefore, the G-BiLayer-GRU employs a dynamic adjustment mechanism, that is, the input historical trajectory data is updated at each sampling point to adjust the latest prediction results adaptively. In order to demonstrate this dynamic adjustment process concretively, this paper selects a typical shifting left trajectory time sequence from the test set. Figure 10 shows the trajectory distribution prediction of target vehicle and real-time changes of RMSE/ADE of each comparison model under six t_{pred} conditions above,

TABLE 4. Prediction index data of different trajectory models.

Advanced prediction intervals	Evaluation index	Trajectory prediction models					
		G-BiLayer-GRU	Triple layer GRU	LSTM-BiLayer-GRU	BiLayer-LSTM	Tri-LSTM	LSTM-RBF
t_{pred}= 0.0 s	RMSE/m	1.46	3.80	2.91	2.46	2.58	2.77
	ADE/m	1.25	3.56	2.69	1.91	2.43	2.40
	FDE/m	2.79	5.92	4.38	6.56	4.65	4.44
	PTC/ms	76.59	80.13	81.94	91.22	109.23	475.11
t_{pred} = 1.0 s	RMSE/m	1.72	4.74	3.59	2.54	2.63	3.07
	ADE/m	1.51	4.42	3.35	2.19	2.38	2.75
	FDE/m	3.56	7.34	5.44	6.68	4.66	5.71
	PTC/ms	79.23	84.28	92.91	99.20	111.85	539.43
t_{pred} = 1.5s	RMSE/m	1.77	5.01	3.72	2.78	2.96	3.25
	ADE/m	1.59	4.65	3.45	2.48	2.65	2.97
	FDE/m	3.57	7.83	5.80	7.00	4.84	6.11
	PTC/ms	81.32	89.48	95.35	107.41	118.45	573.35
t_{pred} = 2 .0s	RMSE/m	1.81	5.22	3.80	2.94	3.16	3.37
	ADE/m	1.62	4.83	3.48	2.64	2.85	3.11
	FDE/m	4.42	8.25	6.11	7.33	5.05	6.44
	PTC/ms	84.78	94.29	99.55	112.50	126.54	617.02
t_{pred} = 2.5s	RMSE/m	1.85	5.41	3.85	3.01	3.19	3.46
	ADE/m	1.61	4.95	3.44	2.67	2.94	3.22
	FDE/m	3.95	8.69	6.44	7.72	5.29	6.79
	PTC/ms	88.34	99.24	106.89	118.46	138.92	675.29
t_{pred} = 3.0 s	RMSE/m	1.88	5.64	3.96	3.05	3.19	3.49
	ADE/m	1.60	5.15	3.47	2.64	2.97	3.25
	FDE/m	5.36	9.10	6.74	8.07	5.54	7.11
	PTC/ms	92.10	105.24	112.43	125.26	144.65	738.47

which can directly reflect the real-time position relationship between the real trajectory of target vehicle and the predicted trajectory.

In the evaluation indexes of real-time trajectory prediction, both RMSE and ADE are used to measure the average difference between the predicted trajectory and the real trajectory, and they are essentially equivalent. According to the analysis of Figure 10, The graph of RMSE and ADE for G-BiLayer-GRU model is always positioned below the graphs of other models, which shows that the precision, stability and robustness of G-BiLayer-GRU model in real-time state are significantly better than those of other five models.

The information of error and prediction time consuming for different prediction models at different t_{pred} times is shown in Table 4 and Figure 11. The RMSE, ADE and FDE indexes of each prediction model in different advanced prediction intervals are compared and analyzed, which is helpful to comprehensively evaluate the performance of the model, and the prediction time consuming indexes are helpful to make a trade-off between accuracy and efficiency.

In Table 4, Figures 11 and 12, RMSE, ADE and FDE index values of all trajectory prediction models show an upward trend with the increase of t_{pred} value, indicating that the difficulty of prediction increases with the increase of time. G-BiLayer-GRU and BiLayer-LSTM models perform well and are significantly superior to other models in various indexes, especially with short advanced prediction interval. The prediction time consumption of LSTM-RBF model

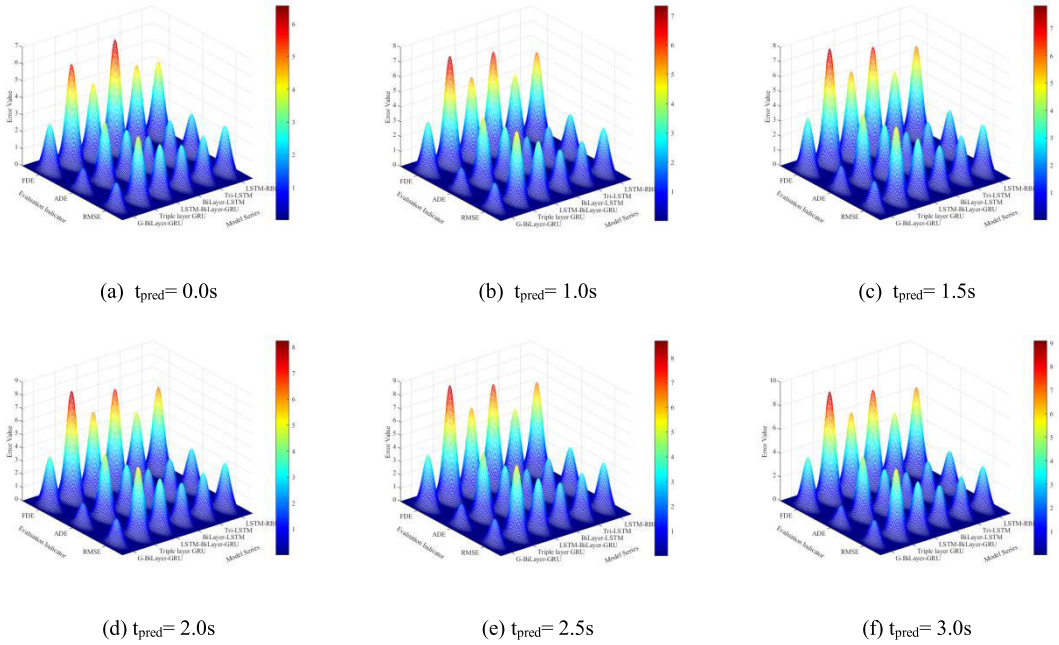

(a) t_{pred}= 0.0s (b) t_{pred}= 1.0s (c) t_{pred}= 1.5s

(d) t_{pred}= 2.0s (e) t_{pred}= 2.5s (f) t_{pred}= 3.0s

FIGURE 11. Distribution of trajectory prediction error indexes of different models.

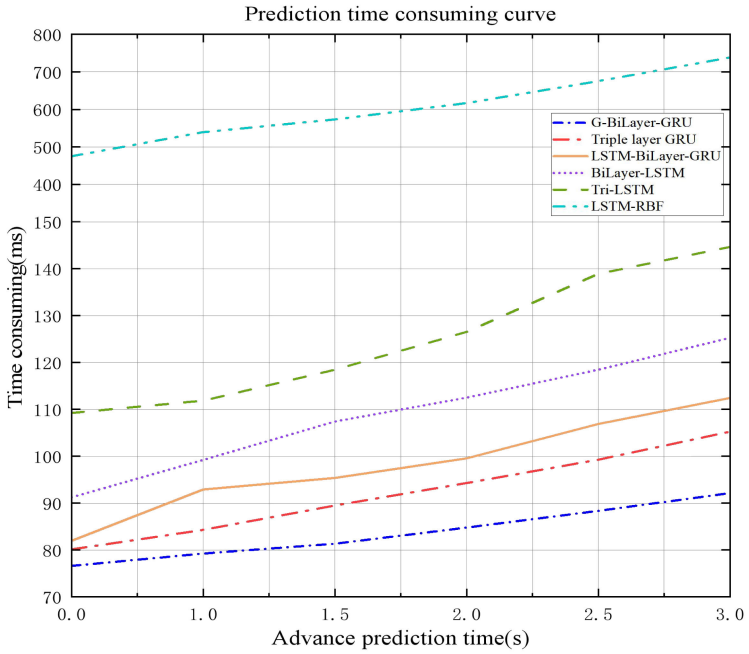

FIGURE 12. Prediction time consuming curve of different models for trajectory prediction.

is significantly more than that of other models, several times or even ten times, which is related to its complex modeling process. The performance of G-BiLayer-GRU and BiLayer-LSTM models is more balanced in various indexes, which not only ensures the prediction accuracy, but also controls the prediction time consuming. In contrast, Tri-LSTM and LSTM-RBF models have shortcomings in accuracy and efficiency. G-BiLayer-GRU model combines the lane change prediction results and the double-gated cycle unit structure, and exhibits the most excellent performance in the vehicle trajectory prediction task, with good prediction accuracy, small prediction deviation and high computational efficiency, and can most vividly ''restore'' the real trajectory of the target vehicle in the actual traffic environment. It can improve the driving safety of AVs in the high-speed traffic flow environment.

VII. CONCLUSION

This paper presents the LSTM-GAT-Bilayer-GRU hybrid prediction model, a novel approach harnessing deep learning techniques to enhance predictive accuracy and real-time responsiveness in dynamic traffic environments. The LSTM-GAT-Bilayer-GRU consists of a vehicle lane change prediction model (LSTM-GAT) and a trajectory prediction model (G-BiLayer-GRU), which has demonstrated itself remarkable efficacy in processing complex vehicular interactions and environmental dynamics in human-machine mixed driving traffic flow. The Lstm-GAT model performs well in processing time sequence data and capturing long-term dependencies, and significantly improves the accuracy and robustness of lane change intent prediction by weighting key features through the graph attention mechanism. For the prior information of lane change intention prediction combined from LSTM-GAT model, G-BiLayer-GRU model represents the highest precision prediction and the lowest prediction time consuming under different advanced prediction intervals, showing good ability of high precision, stability and real-time dynamic adjustment in vehicle trajectory prediction. After undergoing numerical experiment verification, the LSTM-GAT-Bilayer-GRU model proposed in this paper has fully demonstrated its effectiveness and reliability. This accomplishment not only presents novel perspectives for research in AVs and intelligent transportation but also boosts the application of deep learning in these domains. The study elevates the intelligent perception and decision-making capabilities, empowering AVs to swiftly and precisely anticipate lane changes and driving trajectories of neighboring vehicles amidst dynamic and intricate traffic patterns, promising safer and more efficient navigation in real-world scenarios, expected to provide substantial support for optimizing traffic quality, preventing traffic accidents and comprehensively promoting intelligent transportation.

Although our research offers significant contributions, we must also acknowledge its limitations, such as the fact that our proposed model does not consider factors such as vehicle dynamics, vehicle dimension, and sudden road conditions. Future research could further enhance our model by incorporating factors such as denser neighboring vehicles, weather conditions, road infrastructure, and traffic regulations. Furthermore, improving the model's efficiency would enable its application in a wider range of fields, such as smart cities, intelligent transportation systems, and autonomous logistics, bringing greater efficiency and safety to these areas.

REFERENCES

[1] Y. Ma, Z. Wang, H. Yang, and L. Yang, "Artificial intelligence applications in the development of autonomous vehicles: A survey," *IEEE/CAA J. Autom. Sinica*, vol. 7, no. 2, pp. 315–329, Mar. 2020.

[2] A. Aluja, F. Balada, O. García, and L. F. García, "Psychological predictors of risky driving: The role of age, gender, personality traits (Zuckerman's and gray's models), and decision-making styles," *Frontiers Psychol.*, vol. 14, May 2023, Art. no. 1058927.

[3] Y. Liu and X. Wang, "Differences in driving intention transitions caused by Driver's emotion evolutions," *Int. J. Environ. Res. Public Health*, vol. 17, no. 19, p. 6962, Sep. 2020.

[4] P. Hang, C. Lv, C. Huang, J. Cai, Z. Hu, and Y. Xing, "An integrated framework of decision making and motion planning for autonomous vehicles considering social behaviors," *IEEE Trans. Veh. Technol.*, vol. 69, no. 12, pp. 14458–14469, Dec. 2020.

[5] M. Al-Nuaimi, S. Wibowo, H. Qu, J. Aitken, and S. Veres, "Hybrid verification technique for decision-making of self-driving vehicles," *J. Sensor Actuator Netw.*, vol. 10, no. 3, p. 42, Jun. 2021.

[6] J. Lisheng, H. Guangde, X. Xian-Yi, G. Bo-Cang, L. Guo-Feng, and Z. Wen-Tao, "Review of autonomous driving decision making based on reinforcement learning," *Automot. Eng.*, vol. 45, no. 4, pp. 527–540, 2023.

[7] A. Kesting, M. Treiber, and D. Helbing, "General lane-changing model MOBIL for car-following models," *Transp. Res. Rec., J. Transp. Res. Board*, vol. 1999, no. 1, pp. 86–94, Jan. 2007.

[8] S. Moridpour, M. Sarvi, G. Rose, and E. Mazloumi, "Lane-changing decision model for heavy vehicle drivers," *J. Intell. Transp. Syst.*, vol. 16, no. 1, pp. 24–35, Jan. 2012.

[9] C. Xu, W. Zhao, and C. Wang, "An integrated threat assessment algorithm for decision-making of autonomous driving vehicles," *IEEE Trans. Intell. Transp. Syst.*, vol. 21, no. 6, pp. 2510–2521, Jun. 2020.

[10] X. Cao, "Motion control and decision planning for car following and lane changing of autonomous vehicle," Jilin Univ., Changchun, China, Tech. Rep., vol. 2023, pp. 84–90, doi: 10.27162/d.cnki.gjlin.2022.001243.

[11] Y. Wang, C. Wang, W. Zhao, and C. Xu, "Decision-making and planning method for autonomous vehicles based on motivation and risk assessment," *IEEE Trans. Veh. Technol.*, vol. 70, no. 1, pp. 107–120, Jan. 2021.

[12] Y. Jeong, "Predictive lane change decision making using bidirectional long shot-term memory for autonomous driving on highways," *IEEE Access*, vol. 9, pp. 144985–144998, 2021.

[13] W. Hu, Z. Deng, D. Cao, B. Zhang, A. Khajepour, L. Zeng, and Y. Wu, "Probabilistic lane-change decision-making and planning for autonomous heavy vehicles," *IEEE/CAA J. Autom. Sinica*, vol. 9, no. 12, pp. 2161–2173, Dec. 2022.

[14] E. C. Akrida, G. B. Mertzios, P. G. Spirakis, and V. Zamaraev, "Temporal vertex cover with a sliding time window," *J. Comput. Syst. Sci.*, vol. 107, pp. 108–123, Feb. 2020.

[15] R. Krajewski, J. Bock, L. Kloeker, and L. Eckstein, "The highD dataset: A drone dataset of naturalistic vehicle trajectories on German highways for validation of highly automated driving systems," in *Proc. 21st Int. Conf. Intell. Transp. Syst. (ITSC)*, Nov. 2018, pp. 2118–2125.

[16] C. Chiarella, X.-Z. He, and C. Hommes, "A dynamic analysis of moving average rules," *J. Econ. Dyn. Control*, vol. 30, nos. 9–10, pp. 1729–1753, Sep. 2006.

[17] J. Ledolter, "Smoothing time series with local polynomial regression on time," *Commun. Statist.-Theory Methods*, vol. 37, no. 6, pp. 959–971, Feb. 2008.

[18] T. Guo, T. Zhang, E. Lim, M. López-Benítez, F. Ma, and L. Yu, "A review of wavelet analysis and its applications: Challenges and opportunities," *IEEE Access*, vol. 10, pp. 58869–58903, 2022.

[19] M. Khodarahmi and V. Maihami, "A review on Kalman filter models," *Arch. Comput. Methods Eng.*, vol. 30, no. 1, pp. 727–747, 2023.

[20] A. Gomaa, T. Minematsu, M. M. Abdelwahab, M. Abo-Zahhad, and R.-I. Taniguchi, "Faster CNN-based vehicle detection and counting strategy for fixed camera scenes," *Multimedia Tools Appl.*, vol. 81, no. 18, pp. 25443–25471, Jul. 2022.

[21] J. Shi and C. Liu, "NGSIM vehicle trajectory reconstruction," *J. Beijing Univ. Technol.*, vol. 45, no. 6, pp. 1–27, 2019.

[22] Y.-N. Ma, W. Jiang, J.-Y. Wu, J.-Y. Chen, N. Li, Z.-G. Xu, and L. Xiong, "Self-evolution scenarios for simulation tests of autonomous vehicles based on different models of driving styles," *China J. Highway Transp.*, vol. 36, no. 2, pp. 216–220, 2023, doi: 10.19721/j.cnki.1001-7372.2023.02.018.

[23] Editorial Department of China Journal of Highway and Transport, "Review on China's traffic engineering research progress: 2016," *China J. Highway Transp.*, vol. 29, no. 6, pp. 3–9, 2016, doi: 10.19721/j.cnki.1001-7372.2016.06.001.

[24] K. Xu, J. Ba, R. Kiros, K. Cho, A. Courville, R. Salakhudinov, R. Zeme, and l Y. Bengio, "Show, attend and tell: Neural image caption generation with visual attention," in *Proc. Int. Conf. Mach. Learn.*, 2015, pp. 2048–2057.

[25] J.-B. Cordonnier, A. Loukas, and M. Jaggi, "Multi-head attention: Collaborate instead of concatenate," 2020, *arXiv:2006.16362*.

[26] R. Schubert, C. Adam, M. Obst, N. Mattern, V. Leonhardt, and G. Wanielik, "Empirical evaluation of vehicular models for ego motion estimation," in *Proc. IEEE Intell. Vehicles Symp. (IV)*, Jun. 2011, pp. 534–539.
[27] L. Li, G. Sun, and J. Song, "Target trajectory prediction based on neural network and Kalman filtering," in *Optics and Photonics*, vol. 11342. Bellingham, WA, USA: SPIE, 2019, pp. 127–135.
[28] J. A. Hartigan, *Bayes Theory*. Cham, Switzerland: Springer, 2012.
[29] B. Charbuty and A. Abdulazeez, "Classification based on decision tree algorithm for machine learning," *J. Appl. Sci. Technol. Trends*, vol. 2, no. 1, pp. 20–28, Mar. 2021.
[30] D. Mustafa Abdullah and A. Mohsin Abdulazeez, "Machine learning applications based on SVM classification a review," *Qubahan Academic J.*, vol. 1, no. 2, pp. 81–90, Apr. 2021.
[31] R. Genuer and J.-M. Poggi, *Random Forests*. Cham, Switzerland: Springer, 2020, pp. 33–55.
[32] I. Markoulidakis, G. Kopsiaftis, I. Rallis, and I. Georgoulas, "Multi-class confusion matrix reduction method and its application on net promoter score classification problem," in *Proc. 14th Pervasive Technol. Rel. Assistive Environments Conf.*, Jun. 2021, pp. 412–419.
[33] R. K. Shukla and A. K. Tiwari, "Comparative analysis of machine learning based approaches for face detection and recognition," *J. Inf. Technol. Manag.*, vol. 13, no. 1, pp. 1–21, 2021.
[34] J. Wang, L. Sun, H. Li, R. Ding, and N. Chen, "Prediction model of fouling thickness of heat exchanger based on TA-LSTM structure," *Processes*, vol. 11, no. 9, p. 2594, Aug. 2023.
[35] J. Zhang, Y. Xie, K. Li, Z. Wang, and W. Du, "Hierarchical decoding with latent context for image captioning," *Neural Comput. Appl.*, vol. 35, no. 3, pp. 2429–2442, Jan. 2023.
[36] H. Liu, B. He, P. Qin, X. Zhang, S. Guo, and X. Mu, "Sea level anomaly intelligent inversion model based on LSTM-RBF network," *Meteorol. Atmos. Phys.*, vol. 133, no. 2, pp. 245–259, Apr. 2021.

LEI WANG received the B.S. and M.S. degrees from the School of Automobile, Chang'an University, China, where he is currently pursuing the Ph.D. degree in vehicle application engineering. He was an Assistant Professor with the School of Automobile & Rail Transportation, Sino-German University of Applied Sciences, China. He has been presided over and participated in more than ten scientific research projects from government, research institutions, and enterprises. He has also published over 15 papers and eight inventions have been authorized. His current research interests include autonomous driving, vehicle road collaboration technology, and traffic safety theory.

JIANYOU ZHAO received the Ph.D. degree from Chang'an University, China. He is currently a Professor and a Doctoral Supervisor with Chang'an University. He has been an Assistant Professor with the Mechanical Engineering Department, Texas A&M University, College Station. He has published more than 150 articles in authoritative Chinese journals and international journals. His 70 inventions have been authorized. He has been presided over and participated in more than 20 scientific research projects from the Natural Science Foundation, State 863 Plan Project, and Western Transportation. He has won three provincial awards and six national patents. He is a member of China Society of Automobile, China Society of Human Engineering, Shaanxi Highway Society, and China Library Society.

MEI XIAO received the Ph.D. degree from Xi'an Jiaotong University, China. She is currently the Director of the Institute of Transportation Big Data and Artificial Intelligence, Chang'an University, a Professor/Doctoral Supervisor, and a Responsible Professor in the transportation major (a National Brand Major). She has presided over eight scientific research projects with national and provincial level and won two awards of Provincial Science and Technology Progress. She has published over 50 articles and 20 inventions have been authorized. Her current research interests include traffic planning and management, traffic organization and control, intelligent transportation systems, video image processing, and information fusion algorithms.

JIAN LIU is currently pursuing the bachelor's degree with the School of Automobile & Rail Transportation, Sino-German University of Applied Sciences, China. He participated in the 2022 China Intelligent Connected Vehicle (ICV) Algorithm Competition and the 2023 World Autonomous Driving Challenge (Metaverse Simulation Competition). His current research interests include mathematical modeling and computer programming.